

[(2-(Trimethylammonium)ethyl)cyclopentadienyl]tricarbonylmetalates: Group VI Metal Zwitterions

Paul J. Fischer,*[†] Zoey R. Herm,[†] and Benjamin E. Kucera[‡]

Department of Chemistry, Macalester College, Saint Paul, Minnesota 55105-1899, and Department of Chemistry, X-ray Crystallographic Laboratory, University of Minnesota, Minneapolis, Minnesota 55455-0431

Received May 19, 2007

Summary: Zwitterionic [(2-(trimethylammonium)ethyl)cyclopentadienyl]tricarbonylmetalates, $M(\text{CO})_3(\eta^5\text{-Cp}^{\text{NMe}})$ ($M = \text{Cr}$ (7), Mo (8), W (9)), provide useful models to assess intramolecular through-space electrostatic interactions on the reactivity of formally negatively charged metals. The C_{3v} $M(\text{CO})_3$ units in these zwitterions appear largely unperturbed by the tethered 2-(trimethylammonium)ethyl group; neither significant intra- nor intermolecular ion pairing occurs either in solution or in the solid state. Although the donor ability of the Cp group in these zwitterions is essentially identical with that in $[M(\text{CO})_3(\eta^5\text{-Cp})]^-$ on the basis of spectroscopic and crystallographic data, the metal-based reactivity of 7–9 appears to be decreased relative to that of $[M(\text{CO})_3(\eta^5\text{-Cp})]^-$. While the latter reacts with HCl, AuPPh_3Cl , CH_3I , and I_2 to provide robust $M(\text{II})$ complexes, isolable products could only be obtained from reactions of 7–9 with I_2 and CH_3I . One important strategy in the design of zwitterionic organometalates is that metal-based reactivity is enhanced as the tethered counterion steric bulk increases to decrease significant ion-pairing interactions. The relative inertness of 7–9 compared to their protonated analogues $M(\text{CO})_3(\eta^5\text{-Cp}^{\text{NH}})$, despite the absence of structural perturbations in 7–9 due to ion pairing, indicates that ion-pairing interactions are not the only important factors that determine metal-based reactivity in organometallic zwitterions.

The design of organometallic zwitterions for catalytic applications¹ and as building blocks for metallodendritic assemblies² is an active research area. The potential of tuning the reactivity of metal centers by incorporating an intramolecular charge separation motivates these studies. Two strategies have emerged to rationally modulate the steric and electronic metal environment in organometallic zwitterions with covalently interconnected cationic and anionic sites. Either the tether length or substituents at the charged sites can be varied. One strategy that informs the design of zwitterionic organometalates is that metal-based reactivity is enhanced as tethered counterion steric bulk increases to decrease significant ion-pairing interactions. Few organometallic zwitterions with formally anionic metal centers have been reported, despite speculation that intramo-

lecular through-space electrostatic interactions in the coordination sphere of reduced metal centers could modulate catalyst activity and selectivity.³

Baird recently reported group VI metal carbonyls of methyldiphenylphosphonium cyclopentadienyliide, $M(\text{CO})_3(\eta^5\text{-C}_5\text{H}_4\text{-PMePh}_2)$ ($M = \text{Cr}$ (1), Mo (2), W (3)).⁴ This ligand exhibits considerable zwitterionic character in its electronic ground state, and its donor ability toward $M(\text{CO})_3$ fragments was classified as less than that of cyclopentadienyl anion but much greater than that of benzene. Spectroscopic and reactivity comparisons to $[M(\text{CO})_3(\eta^5\text{-Cp})]^-$ were instrumental for this determination. While the zwitterionic resonance forms of 1–3 feature an implied cyclopentadienyl anion-like structure that is expected to be a stronger donor than $\eta^6\text{-benzene}$, they also feature a through-space electrostatic interaction between a formally positively charged phosphorus atom and formally negatively charged metal centers. The impact of related through-space interactions on formally charged metals is often significant. Despite the formal negative charge on tungsten in the zwitterionic olefin-coordinated imine complex $\text{W}(\text{CO})_2(\eta^2\text{-Z})\text{-}(\text{Me}_2\text{N}=\text{C}(\text{Me})\text{CH}=\text{CHCOOH})(\eta^5\text{-Cp})$, the metal neither deprotonates the carboxylic acid nor is methylated by CH_3I .^{3b,5} On the basis of the significant role that intramolecular through-space electrostatic interactions have in zwitterionic organometalates, it would be of interest to compare 1–3 to corresponding $M(\text{CO})_3$ complexes with formally unambiguous Cp donation, but containing through-space electrostatic interactions due to intramolecular ion pairing.

The (2-(dimethylamino)ethyl)cyclopentadienyl (Cp^{N}) group VI metal carbonyl anions⁶ seemed excellent precursors to such complexes. Protonation of these anions proceeds at the amine to afford zwitterionic [(2-(dimethylammonium)ethyl)cyclopentadienyl]tricarbonylmetalates, $M(\text{CO})_3(\eta^5\text{-Cp}^{\text{NH}})$ ($M = \text{Cr}$ (4), Mo (5), W (6)), which engage in $\text{N}\cdots\text{H}\cdots\text{M}$ hydrogen bonding.⁷ The interaction between the separated charges distorts the $M(\text{CO})_3$ fragments and renders the formally negatively charged metal centers less reactive than those in $[M(\text{CO})_3(\eta^5\text{-Cp})]^-$. In an effort to more closely model the through-space interaction in 1–3 that does not feature structural perturbations due to ion pairing, we synthesized the methylated zwitterions $M(\text{CO})_3(\eta^5\text{-Cp}^{\text{NMe}})$. Spectroscopic and reactivity studies were subsequently carried out to assess the $M(\text{CO})_3(\eta^5\text{-Cp}^{\text{NMe}})$ $M(\text{CO})_3$ fragment electronic environment relative to 1–3 and 4–6 afforded by modification of the pendant ammonium ion.

* To whom correspondence should be addressed. E-mail: fischer@macalester.edu.

[†] Macalester College.

[‡] University of Minnesota.

(1) (a) Piers, W. E. *Chem. Eur. J.* **1998**, *4*, 13. (b) Piers, W. E.; Sun, Y.; Lee, L. W. M. *Top. Catal.* **1999**, *7*, 133. (c) Bochmann, M. *Top. Catal.* **1999**, *7*, 9. (d) Thorn, M. G.; Etheridge, Z. C.; Fanwick, P. E.; Rothwell, I. P. *Organometallics* **1998**, *17*, 3636. (e) Zhou, Z.; Facey, G.; James, B. R.; Alper, H. *Organometallics* **1996**, *15*, 2496. (f) Zhou, Z.; James, B. R.; Alper, H. *Organometallics* **1995**, *14*, 4209. (g) Zhou, J.-Q.; Alper, H. *Organometallics* **1994**, *13*, 1586. (h) van der Heijden, H.; Hessen, B.; Orpen, A. G. *J. Am. Chem. Soc.* **1998**, *120*, 1112. (i) Lu, C. C.; Peters, J. C. *J. Am. Chem. Soc.* **2002**, *124*, 5272. (j) Betley, T.; Peters, J. C. *Inorg. Chem.* **2002**, *41*, 6541. (k) Bianchini, C.; Meli, A.; Patinec, V.; Sernau, V.; Vizza, F. *J. Am. Chem. Soc.* **1997**, *119*, 4945. (l) Amer, I.; Alper, H. *J. Am. Chem. Soc.* **1990**, *112*, 3674. (m) Hlatky, G. G.; Turner, H. W.; Eckman, R. R. *J. Am. Chem. Soc.* **1989**, *111*, 2728.

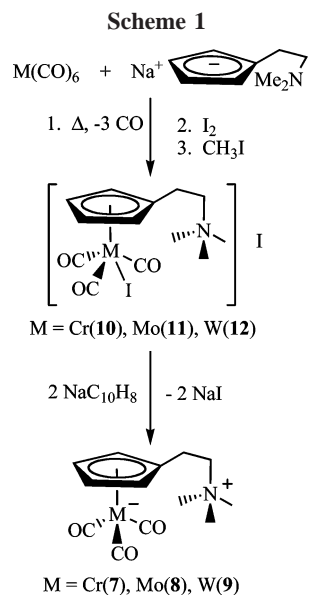
(2) (a) van de Coevering, R.; Kuil, A. P.; Visser, T.; Lutz, M.; Spek, A. L.; Klein Gebbink, R. J. M.; van Koten, G. *Organometallics* **2005**, *24*, 6147. (b) Yang, Q.-Z.; Siri, O.; Braunstein, P. *Chem. Eur. J.* **2005**, *11*, 7237.

(3) (a) Chauvin, R. *Eur. J. Inorg. Chem.* **2000**, 577. (b) Butters, C.; Carr, N.; Deeth, R. J.; Green, M.; Green, S. M.; Mahon, M. F. *J. Chem. Soc., Dalton Trans.* **1996**, 2299. (c) Lee, L.; Chen, D.-J.; Lin, Y.-C.; Lo, Y.-H.; Lin, C. H.; Lee, G.-H.; Wang, Y. *Organometallics* **1997**, *16*, 4636.

(4) Brownie, J. H.; Baird, M. C.; Schmider, H. *Organometallics* **2007**, *26*, 1433.

(5) Lee, L.; Chen, D.-J.; Lin, Y.-C.; Lo, Y.-H.; Lin, C. H.; Lee, G.-H.; Wang, Y. *Organometallics* **1997**, *16*, 4636.

(6) Fischer, P. J.; Krohn, K. M.; Mwenda, E. T.; Young, V. G., Jr. *Organometallics* **2005**, *24*, 1776.



Results and Discussion

Synthesis and Characterization of $M(\text{CO})_3(\eta^5\text{-Cp}^{\text{NMe}})$.

Reactions of in situ $\text{Na}[\text{M}(\text{CO})_3(\eta^5\text{-Cp}^{\text{N}})]$ with iodine, followed by methylation with CH_3I , provided $[\text{M}(\text{CO})_3(\eta^5\text{-Cp}^{\text{NMe}})]\text{I}$. Sodium naphthalene reduction of these salts afforded the target zwitterions (Scheme 1) in moderate yield (30–45%). The diminished yield is primarily attributed to the lack of specificity of $\text{NaC}_{10}\text{H}_8$ as a reducing agent toward **10–12**. Some pendant ammonium ion reduction occurs; $\text{Na}[\text{M}(\text{CO})_3(\eta^5\text{-Cp}^{\text{N}})]$ was spectroscopically identified in each reaction mixture, and residual $[\text{M}(\text{CO})_3(\eta^5\text{-Cp}^{\text{N}})]\text{I}$ remained after all $\text{NaC}_{10}\text{H}_8$ had been consumed. Solution IR $\nu(\text{CO})$ spectra of **1–9** and $[\text{PPN}][\text{M}(\text{CO})_3(\eta^5\text{-Cp}^{\text{N}})]$ ($\text{M} = \text{Cr}$ (**13**), Mo (**14**), W (**15**))⁶ (Table 1) indicate that zwitterionic Cp^{NMe} and anionic Cp^{N} ligands have nearly indistinguishable donor abilities toward $\text{M}(\text{CO})_3$ fragments. The intramolecular charge separation in **7–9** has a modest electronic impact on the basis of these data. The $\nu(\text{CO})$ absorptions of **7–9** are shifted to higher energy by a maximum of 5 cm^{-1} relative to the corresponding absorptions of **13–15**. Zwitterions **7–9** and **1–3** feature unperturbed C_{3v} $\text{M}(\text{CO})_3$ units in solution, like those found in **13–15**, where PPN^+ engages in no significant interactions with the anions. These spectral data for **4–6** indicate perturbation of $\text{M}(\text{CO})_3$ fragments due to hydrogen bonding but may also provide an upper limit for the electronic influence of through-space electrostatic interactions in this class of group VI metal carbonyls. The asymmetric $\nu(\text{CO})$ absorptions of **7–9** are $\sim 9\text{ cm}^{-1}$ lower than the lowest energy $\nu(\text{CO})$ absorptions of **4–6**. These absorptions in **4–6** are $\sim 26\text{ cm}^{-1}$ lower than the lowest energy $\nu(\text{CO})$ absorptions in **1–3**, further emphasizing that the $\eta^5\text{-Cp}$ groups in **4–9** are much better donors than the $\eta^5\text{-C}_5\text{H}_4\text{PMePh}_2$ group in **1–3**.

The three-legged piano-stool structures of **7–9** are displayed in Figures S1 (Supporting Information), 1, and S2, respectively. Zwitterions **7–9** lie on a mirror plane; the pendant ammonium ion occupies space between the carbonyls defined by C(1) and C(1A), and C(3) is opposite the CO defined by C(2). The relative orientation of the 2-(trimethylammonium)ethyl and $\text{M}(\text{CO})_3$ units in **7–9** in the solid state is antiperiplanar, on the basis of

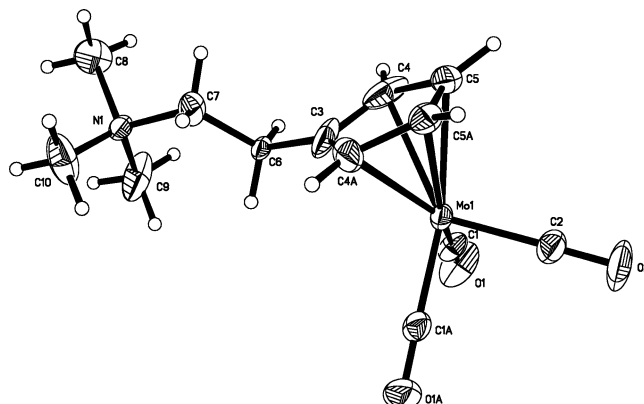


Figure 1. Molecular structure of **8** (50% thermal ellipsoids). Selected bond lengths (Å) and angles (deg): $\text{Mo}-\text{C}(1/1\text{A}) = 1.926(5)$, $\text{Mo}-\text{C}(2) = 1.926(7)$, $\text{Mo}-\text{C}(\text{O})$ (av) = $1.926(7)$, $\text{Mo}-\text{C}(3) = 2.400(7)$, $\text{Mo}-\text{C}(4/4\text{A}) = 2.384(5)$, $\text{Mo}-\text{C}(5/5\text{A}) = 2.378(5)$, $\text{Mo}-\text{C}(\text{dienyl})$ (av) = $2.385(9)$, $\text{C}(1/1\text{A})-\text{O}(1/1\text{A}) = 1.166(6)$, $\text{C}(2)-\text{O}(2) = 1.171(9)$, $\text{C}-\text{O}$ (av) = $1.168(3)$; $\text{C}(2)-\text{Mo}-\text{C}(1/1\text{A}) = 86.5(2)$, $\text{C}(1\text{A})-\text{Mo}-\text{C}(1) = 83.6(3)$, $(\text{O})\text{C}-\text{Mo}-\text{C}(\text{O})$ (av) = $86(2)$, $\text{O}(1/1\text{A})-\text{C}(1/1\text{A})-\text{Mo} = 179.0(4)$, $\text{O}(2)-\text{C}(2)-\text{Mo} = 179.5(7)$, $\text{O}-\text{C}-\text{Mo}$ (av) = $179.2(3)$.

$\text{N}-\text{C}(7)-\text{C}(6)-\text{C}(3)$ torsion angles (**7**, $167.3(3)^\circ$; **8**, $164.5(3)^\circ$; **9**, $164.9(4)^\circ$). The ion pairing has no apparent impact on the structures of the $\text{M}(\text{CO})_3$ fragments, in contrast to the distortions in **4–6**. The unperturbed $\text{M}(\text{CO})_3$ units of **7–9** resemble those of **1–3**. Important average lengths and angles that define the $\text{M}(\text{CO})_3$ fragments of **7–9** ($\text{M}-\text{C}(\text{O})$, $\text{C}-\text{O}$, $(\text{O})\text{C}-\text{M}-\text{C}(\text{O})$, $\text{O}-\text{C}-\text{M}$; averages given in the captions of Figures S1, 1, and S2) are statistically indistinguishable from those of **1–3**, respectively. The average $\text{M}-\text{C}(\text{dienyl})$ lengths of **7–9** (given in the figure captions) are also statistically identical with the corresponding values of **1–3**, respectively. These structural comparisons support the high zwitterionic character proposed for **1–3**.

Reactivity of $\text{M}(\text{CO})_3(\eta^5\text{-Cp}^{\text{NMe}})$. The attenuation of **2** toward oxidative addition relative to $[\text{Mo}(\text{CO})_3(\eta^5\text{-Cp})]^-$ was also used to gauge the zwitterionic character of **2**. While $[\text{Mo}(\text{CO})_3(\eta^5\text{-Cp})]^-$ reacts with CH_3I and I_2 , resulting in $\text{MoCH}_3(\text{CO})_3(\eta^5\text{-Cp})$ and $\text{MoI}(\text{CO})_3(\eta^5\text{-Cp})$, respectively, **2** is inert toward CH_3I but reacts with I_2 to afford $[\text{MoI}(\text{CO})_3(\eta^5\text{-C}_5\text{H}_4\text{PMePh}_2)]\text{I}$ (**16**).⁴ Complexes **7–9** permit the opportunity to probe the reactivity of zwitterionic $\text{M}(\text{CO})_3$ complexes with a substituted Cp group which is a stronger donor than that in **1–3** but also with a through-space ion-pairing interaction devoid of associated structural perturbations (unlike **4–6**). On the basis of parallel reactivity studies (vide infra), zwitterions **7–9** appear more reactive than **1–3** but surprisingly *less* reactive than **4–6** toward oxidative addition. A design assumption associated with zwitterionic organometalate catalysts is that metal-based reactivity is enhanced as tethered counterion bulk increases to attenuate ion-pairing interactions.^{1a} On the basis of this premise, the metal-based reactivity of **7–9** would be expected to be greater than that of **4–6**.

Reactions of **7–9** and I_2 quantitatively afforded isolable samples of **10–12**, respectively, spectroscopically identical in the IR $\nu(\text{CO})$ region with those obtained via Scheme 1. Isolable $[\text{M}'\text{CH}_3(\text{CO})_3(\eta^5\text{-Cp}^{\text{NMe}})]\text{I}$ ($\text{M}' = \text{Mo}$ (**17**), W (**18**)), spectroscopically identical in the IR $\nu(\text{CO})$ region with those obtained

Table 1. $\nu(\text{CO})$ IR Data (cm^{-1}) for $\text{M}(\text{CO})_3(\eta^5\text{-Cp}^{\text{NMe}})$, $\text{M}(\text{CO})_3(\eta^5\text{-Cp}^{\text{NH}})$, $[\text{PPN}][\text{M}(\text{CO})_3(\eta^5\text{-Cp}^{\text{N}})]$, and $\text{M}(\text{CO})_3(\eta^5\text{-C}_5\text{H}_4\text{PMePh}_2)$

M	$\text{M}(\text{CO})_3(\eta^5\text{-Cp}^{\text{NMe}})$ (7–9) ^a	$\text{M}(\text{CO})_3(\eta^5\text{-Cp}^{\text{NH}})$ (4–6) ^a	$[\text{M}(\text{CO})_3(\eta^5\text{-Cp}^{\text{N}})]^-$ (13–15) ^a	$\text{M}(\text{CO})_3(\eta^5\text{-C}_5\text{H}_4\text{PMePh}_2)$ (1–3) ^b
Cr	1894 (s), 1773 (s)	1906 (s), 1805 (m), 1782 (s)	1889 (s), 1771 (s)	1915 (s), 1812 (s)
Mo	1898 (s), 1780 (s)	1911 (s), 1809 (s), 1788 (s)	1893 (s), 1775 (s)	1918 (s), 1812 (s)
W	1892 (s), 1773 (s)	1904 (s), 1803 (s), 1782 (s)	1887 (s), 1770 (s)	1912 (s), 1808 (s)

^a In CH_3CN . ^b In CH_2Cl_2 .

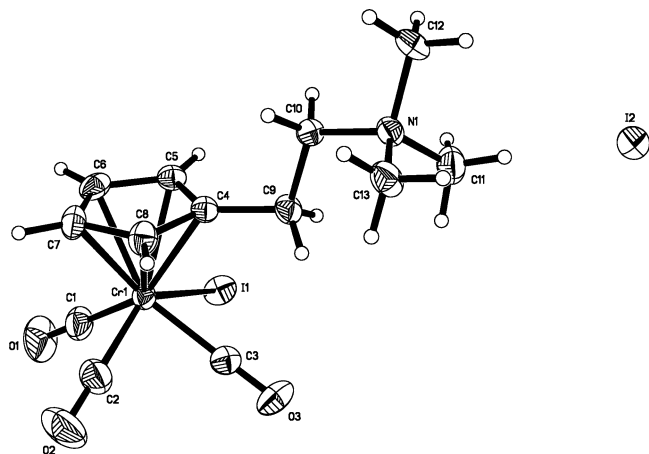


Figure 2. Molecular structure of **10** (50% thermal ellipsoids). Selected bond lengths (Å) and angles (deg): Cr–I(1) = 2.7817(8), Cr–C(1) = 1.887(5), Cr–C(2) = 1.853(6), Cr–C(3) = 1.896(5), Cr–C(4) = 2.205(4), Cr–C(5) = 2.232(4), Cr–C(6) = 2.197(4), Cr–C(7) = 2.170(5), Cr–C(8) = 2.159(5), Cr–C(dienyl) (av) = 2.19(3); C(2)–Cr–I(1) = 131.71(17), C(1)–Cr–C(3) = 116.5(2), C(1)–Cr–I(1) = 75.98(17), C(3)–Cr–I(1) = 74.62(15), C(2)–Cr–C(1) = 80.0(3), C(2)–Cr–C(3) = 79.8(2).

more conveniently via $\text{Na}[\text{M}(\text{CO})_3(\eta^5\text{-Cp}^N)]$, were obtained from reactions of CH_3I with **8** and **9**, respectively. Although aqueous HCl stoichiometrically reacts with **6** to provide $[\text{WH}(\text{CO})_3(\eta^5\text{-Cp}^{\text{NH}})]\text{Cl}$,⁷ attempts to isolate $[\text{MH}(\text{CO})_3(\eta^5\text{-Cp}^{\text{NMe}})]\text{-Cl}$ were uniformly unsuccessful. Aqueous HCl (1 equiv) reacted with **7** and **9** in CH_3CN to afford metal hydride⁸ and starting zwitterion in solution. Excess aqueous HCl (**7**, 5 equiv; **9**, 2 equiv) was required to completely protonate these zwitterions, but removal of this excess resulted in decomposition to **7** and **9**. Reaction of **8** with aqueous HCl (1 equiv) in CH_3CN caused instantaneous formation of $\text{Mo}(\text{CO})_3(\text{CH}_3\text{CN})_3$.⁹ Reaction of **8** with aqueous HCl in THF resembled that of **7** and **9** in $\text{CH}_3\text{-CN}$. Although AuPPh_3Cl reacts with $\text{Na}[\text{M}(\text{CO})_3(\eta^5\text{-Cp}^N)]$ to afford $\text{M}(\text{AuPPh}_3)(\text{CO})_3(\eta^5\text{-Cp}^N)$ ⁷ and with **5** and **6** to provide $[\text{M}''(\text{AuPPh}_3)(\text{CO})_3(\eta^5\text{-Cp}^{\text{NH}})]\text{Cl}$ ($\text{M}'' = \text{Mo}, \text{W}$),⁷ isolable AuPPh_3 derivatives of **7–9** could not be obtained by an analogous direct reaction with AuPPh_3Cl . Methylation of $\text{M}(\text{AuPPh}_3)(\text{CO})_3(\eta^5\text{-Cp}^N)$ with CH_3I (1 equiv) resulted in instantaneous formation of **7–9**, respectively, via reductive elimination.

Characterization of Oxidative Addition Products. The four-legged piano-stool structures of **10–12** are displayed in Figures 2, S3, and S4, respectively. In each structure, the $\eta^5\text{-Cp}$ group is oriented such that the 2-(trimethylammonium)ethyl pendant group occupies space between the iodide ligand and the CO defined by C(3). An antiperiplanar configuration between the 2-(trimethylammonium)ethyl and neutral $\text{MI}(\text{CO})_3$ fragments is present, on the basis of the N–C(10)–C(9)–C(4) torsion angles (**10**, 161.4(4)°; **11**, 162.2(2)°; **12**, 162.1(3)°). These torsion angles are comparable in magnitude to the corresponding angles in **7–9** (vide supra), seemingly independent of the metal formal charge. Complex **10** contains the first structurally characterized $\text{CrI}(\text{CO})_3(\eta^5\text{-Cp})$ fragment. The instability of $\text{CrI}(\text{CO})_3(\eta^5\text{-Cp})$ is well-documented;¹⁰ analytically pure samples of **10** could not be obtained. Monomeric **10** joins the dimer $\text{Cp}_2\text{Cr}_2(\mu\text{-OCMe}_3)_2\text{I}_2$ (**19**)¹¹ and copolymer $\{[\text{Cp}^*\text{CrI}(\mu\text{-I})_2\cdot[\text{Cp}^*\text{Cr}(\text{I}_3)(\mu\text{-I})_2]\}_n$ ¹² as the only crystallographically characterized CpCrIL_3 complexes. The Cr–I length of **10** is significantly longer ($\sim 17\sigma$) than the average Cr–I length of **19** (2.714(4) Å), consistent with the larger Cr(II) radius relative to Cr(III). The average M–C(dienyl) length of **11** and **12** (2.33(4) Å) is essentially uniform with the corresponding average length found in **16** (2.33(3) Å). This is consistent with the increase in aromatic character of the C_5H_4 ring proposed in **2** upon oxidation of the metal, even though the IR $\nu(\text{CO})$ absorptions for **16** in solution are shifted to higher energy by 16 and 20 cm^{-1} , respectively, compared to those of **11**.

The four-legged piano-stool structure of **18** is shown in Figure S5. The $\eta^5\text{-Cp}$ ring is oriented to permit the 2-(trimethylammonium)ethyl substituent to occupy space between the CO defined by C(1) and methyl carbon C(4). Important lengths and angles that define the $\text{WCH}_3(\text{CO})_3$ fragment of **18** (e.g., trans W–C(O), cis W–C(O), trans Me–W–C(O), trans (O)C–W–C(O), cis Me–W–C(O), cis O(C)–W–C(O)) are statistically identical with average values found in $\text{WCH}_3(\text{CO})_3(\eta^5\text{-C}_5\text{H}_4\text{C}(\text{O})\text{ONC}_4\text{H}_4\text{O}_2)$ ¹³ and $(\text{CH}_3)(\text{CO})_3\text{W}[\eta^5\text{-C}_5\text{H}_4\text{-}\{\eta^5\text{-C}_6\text{H}_6\}\text{-Mn}(\text{CO})_3]$.¹⁴ The average W–C(dienyl) distances (**18**, 2.34(1) Å) of these complexes are also statistically indistinguishable. The W–CH₃ length of **18** (2.368(14) Å) is significantly longer (5σ) than the average corresponding distance found in the related complexes, but the absolute difference is small (0.068 Å).

Concluding Remarks. Zwitterionic organometalates with formally negatively charged metals constitute an emerging area of research, and the influence of intramolecular charge separation on metal-based reactivity is a general theme of these investigations. Due to the well-established chemistry of $[\text{M}(\text{CO})_3(\eta^5\text{-Cp})]^-$, analogues containing this fragment have been synthesized to investigate zwitterionic species. Zwitterions **7–9** permit the assessment of intramolecular through-space electrostatic interactions on metal-based reactivity where the substituted Cp groups are as strongly donating as Cp and structural perturbations of the $\text{M}(\text{CO})_3$ units are absent. The IR $\nu(\text{CO})$ spectroscopic data and enhanced metal-based reactivity of **7–9** relative to that of **1–3** underscore the rather weak donor ability of the $\eta^5\text{-C}_5\text{H}_4\text{PMePh}_2$ ligand in **1–3**. The inertness of **7–9** relative to **4–6**, despite the absence of structural perturbations due to ion pairing in **7–9**, indicates that ion-pairing interactions are not the only factors that contribute to metal-based reactivity in organometallic zwitterions. The inertness of **1–9** relative to $\text{Na}[\text{M}(\text{CO})_3(\eta^5\text{-Cp})]$ emphasizes the importance of salt elimination as a contribution to the driving force for formation of $\text{MR}(\text{CO})_3(\eta^5\text{-Cp})$ via reactions of these anions and RX. Precipitation of alkali-metal salts does not accompany these reactions of **1–9**. Further studies of transition-metal complexes containing Cp^N and related ligands are underway in this laboratory.

Experimental Section

Similar procedures were conducted to synthesize **7–9**, **10–12**, and **17–18**, respectively. Representative procedures for **7**, **11**, and **18** are provided below. General procedures and complete experimental details for **8–10**, **12**, and **17** are given in the Supporting Information.

Cr(CO)₃(η⁵-Cp^{NMe}) (7). THF (160 mL) was added to Na (0.253 g, 11.0 mmol) and C_{10}H_8 (2.75 g, 21.5 mmol); the deep green solution was stirred for 3 h. This solution was added to a suspension

(7) Fischer, P. J.; Krohn, K. M.; Mwenda, E. T.; Young, V. G., Jr. *Organometallics* **2005**, *24*, 5116.

(8) The product IR $\nu(\text{CO})$ absorptions were very similar to those of $\text{M}'\text{H}(\text{CO})_3(\eta^5\text{-Cp})$ ($\text{M}' = \text{Cr}, \text{W}$): Jordon, R. F.; Norton, J. R. *J. Am. Chem. Soc.* **1982**, *104*, 1255.

(9) Kubas, G. J.; Kiss, G.; Hoff, C. D. *Organometallics* **1991**, *10*, 2870.

(10) (a) Manning, A. R.; Thornhill, D. J. *J. Chem. Soc. A* **1971**, 637. (b) King, R. B.; Efraty, A.; Douglas, W. M. *J. Organomet. Chem.* **1973**, *60*, 125.

(11) Nefedov, S. E.; Pasynskii, A. A.; Eremenko, I. L.; Orazsakhov, B.; Ellert, O. G.; Novotortsev, V. M.; Katsner, S. B.; Antsyshkina, A. S.; Porai-Koshits, M. A. *J. Organomet. Chem.* **1988**, *345*, 97.

(12) Morse, D. B.; Rauchfuss, T. B.; Wilson, S. R. *J. Am. Chem. Soc.* **1990**, *112*, 1860.

(13) Gorfli, A.; Salmain, M.; Jaouen, G.; McGlinchey, M. J.; Bennouna, A.; Mousser, A. *Organometallics* **1996**, *15*, 142.

(14) Chung, T.-M.; Chung, Y. K. *Organometallics* **1992**, *11*, 2822.

of $[\text{CrI}(\text{CO})_3(\eta^5\text{-Cp}^{\text{NMMe}})]\text{I}$ (2.90 g, 5.36 mmol) in THF (90 mL). The suspension was stirred for 11 h, yielding a brown suspension. A pale green solid was collected by filtration, washed with cold CH_3CN (0 °C, 2×40 mL) to remove trace $[\text{CrI}(\text{CO})_3(\eta^5\text{-Cp}^{\text{NMMe}})]\text{I}$, washed with THF (2×20 mL), and dried in vacuo. The solid was dissolved in hot CH_3CN (75–80 °C, 350 mL) and the solution filtered hot through alumina. Concentration of the filtrate in vacuo to ~5 mL resulted in precipitation of a sparkling yellow solid. Addition of Et_2O (100 mL) precipitated more solid. The bright yellow, air-sensitive microcrystals (0.838 g, 54%) were isolated by filtration, washed with Et_2O (4×10 mL), and dried in vacuo. Anal. Calcd for $\text{C}_{13}\text{H}_{17}\text{NO}_3\text{Cr}$: C, 54.35; H, 5.96; N, 4.88. Found: C, 54.33; H, 5.77; N, 4.91. Mp: 250–253 °C dec. IR (CH_3CN): $\nu(\text{CO})$ 1894 (s), 1773 (s) cm^{-1} . IR (CH_2Cl_2): $\nu(\text{CO})$ 1888 (s), 1770 (s) cm^{-1} . IR (Nujol): $\nu(\text{CO})$ 1901 (s), 1759 (s) cm^{-1} . ^1H NMR ($\text{DMSO}-d_6$, 300 MHz): δ 4.37 (app t, $J = 2.3$ Hz, 2H, Cp), 4.30 (app t, $J = 2.1$ Hz, 2H, Cp), 3.41–3.36 (m, 2H, $\text{CH}_2\text{CH}_2\text{N}$), 3.06 (s, 9H, CH_3), 2.63–2.58 (m, 2H, $\text{CH}_2\text{CH}_2\text{N}$). $^{13}\text{C}\{^1\text{H}\}$ NMR ($\text{DMSO}-d_6$, 75 MHz): δ 245.1 (s, CO).

$[\text{Mo}(\text{CO})_3(\eta^5\text{-Cp}^{\text{NMMe}})]\text{I}$ (8). Yield: 44%. Anal. Calcd for $\text{C}_{13}\text{H}_{17}\text{NO}_3\text{Mo}$: C, 47.14; H, 5.17; N, 4.23. Found: C, 47.21; H, 5.03; N, 4.43. Mp: 261–263 °C dec. IR (CH_3CN): $\nu(\text{CO})$ 1898 (s), 1780 (s) cm^{-1} . IR (Nujol): $\nu(\text{CO})$ 1906 (s), 1774 (s) cm^{-1} . ^1H NMR ($\text{DMSO}-d_6$, 300 MHz): δ 5.03 (app t, $J = 1.8$ Hz, 2H, Cp), 4.94 (app t, $J = 2.3$ Hz, 2H, Cp), 3.39–3.33 (m, 2H, $\text{CH}_2\text{CH}_2\text{N}$), 3.06 (s, 9H, CH_3), 2.71–2.66 (m, 2H, $\text{CH}_2\text{CH}_2\text{N}$). $^{13}\text{C}\{^1\text{H}\}$ NMR ($\text{DMSO}-d_6$, 75 MHz): δ 234.8 (s, CO).

$[\text{W}(\text{CO})_3(\eta^5\text{-Cp}^{\text{NMMe}})]\text{I}$ (9). Yield: 31%. Anal. Calcd for $\text{C}_{13}\text{H}_{17}\text{NO}_3\text{W}$: C, 37.25; H, 4.09; N, 3.34. Found: C, 37.19; H, 3.85; N, 3.36. Mp: 255–256 °C dec. IR (CH_3CN): $\nu(\text{CO})$ 1892 (s), 1773 (s) cm^{-1} . IR (DMSO): $\nu(\text{CO})$ 1887 (s), 1773 (s) cm^{-1} . IR (Nujol): $\nu(\text{CO})$ 1902 (s), 1772 (s) cm^{-1} . ^1H NMR ($\text{DMSO}-d_6$, 300 MHz): δ 5.07 (app t, $J = 2.1$ Hz, 2H, Cp), 4.98 (app t, $J = 2.3$ Hz, 2H, Cp), 3.40–3.34 (m, 2H, $\text{CH}_2\text{CH}_2\text{N}$), 3.06 (s, 9H, CH_3), 2.77–2.72 (m, 2H, $\text{CH}_2\text{CH}_2\text{N}$). $^{13}\text{C}\{^1\text{H}\}$ NMR ($\text{DMSO}-d_6$, 75 MHz): δ 225.6 (s, CO), ^{183}W – ^{13}C satellites 226.9, 224.3, $^1J_{\text{WC}} = 196$ Hz).

$[\text{CrI}(\text{CO})_3(\eta^5\text{-Cp}^{\text{NMMe}})]\text{I}$ (10). A 2.96 g amount was obtained; the yield was not calculated since analytically pure bulk samples could not be obtained. Anal. Calcd for $\text{C}_{13}\text{H}_{17}\text{NO}_3\text{I}_2\text{Cr}$: C, 28.86; H, 3.17; N, 2.59. Found: C, 29.42; H, 3.29; N, 2.82. Mp: 206–209 °C dec. IR (CH_3CN): $\nu(\text{CO})$ 2028 (s), 1968 (s) cm^{-1} . IR (Nujol): $\nu(\text{CO})$ 2026 (s), 1956 (s), 1897 (m, sh) cm^{-1} . ^1H NMR (CD_3CN , 300 MHz): δ 5.44 (s, br, 2H, Cp), 5.22 (s, br, 2H, Cp), 3.61–3.56 (m, 2H, $\text{CH}_2\text{CH}_2\text{N}$), 3.14 (s, 9H, CH_3), 2.91–2.86 (m, 2H, $\text{CH}_2\text{CH}_2\text{N}$).

$[\text{MoI}(\text{CO})_3(\eta^5\text{-Cp}^{\text{NMMe}})]\text{I}$ (11). THF (150 mL) was added to $\text{Mo}(\text{CO})_6$ (2.53 g, 9.57 mmol) and NaCp^{N} (1.60 g, 10.0 mmol). The yellow solution was refluxed for 15 h. The THF was removed in vacuo, and the residue was dissolved in CH_3CN (100 mL). Iodine (2.43 g, 9.57 mmol) in CH_3CN (100 mL) was added, resulting in a deep red solution; the $[\text{Mo}(\text{CO})_3(\eta^5\text{-Cp}^{\text{N}})]^-$ was consumed within 15 min. A 2.0 M solution of CH_3I in *tert*-butyl methyl ether (8.0 mL, containing 2.3 g, 16 mmol of CH_3I) was added; the resulting solution was stirred for 2 h prior to filtration through alumina. The filtrate was concentrated in vacuo until ~3 mL remained and a significant amount of red solid had precipitated. Addition of THF (100 mL) precipitated more solid. The solid was isolated by filtration, washed with THF (4×20 mL), and dried in vacuo. Recrystallization ($\text{CH}_3\text{CN}/\text{THF}$) provided deep red, moderately air-sensitive microcrystals (3.98 g, 71%). Anal. Calcd for $\text{C}_{13}\text{H}_{17}\text{NO}_3\text{I}_2\text{Mo}$: C, 26.69; H, 2.93; N, 2.39. Found: C, 26.80; H, 3.03; N, 2.48. Mp: 253–254 °C dec. IR (CH_3CN): $\nu(\text{CO})$ 2039 (s), 1959 (s) cm^{-1} . IR (Nujol): $\nu(\text{CO})$ 2038 (s), 1951 (s) cm^{-1} . ^1H NMR (CD_3CN , 300 MHz): δ 5.85 (app t, $J = 2.1$ Hz, 2H, Cp), 5.55 (app t, $J = 2.1$ Hz, 2H, Cp), 3.59–3.53 (m, 2H, $\text{CH}_2\text{CH}_2\text{N}$), 3.13

(s, 9H, CH_3), 3.06–3.00 (m, 2H, $\text{CH}_2\text{CH}_2\text{N}$). $^{13}\text{C}\{^1\text{H}\}$ NMR (CD_3CN , 75 MHz): δ 236.9 (s, *trans* CO), 222.7 (s, *cis* CO).

$[\text{WI}(\text{CO})_3(\eta^5\text{-Cp}^{\text{NMMe}})]\text{I}$ (12). Yield: 78%. Anal. Calcd for $\text{C}_{13}\text{H}_{17}\text{NO}_3\text{I}_2\text{W}$: C, 23.20; H, 2.55; N, 2.08. Found: C, 23.34; H, 2.62; N, 2.18. Mp: 208–211 °C dec. IR (CH_3CN): $\nu(\text{CO})$ 2033 (s), 1944 (s) cm^{-1} . IR (Nujol): $\nu(\text{CO})$ 2017 (m), 1945 (m, sh), 1927 (m) cm^{-1} . ^1H NMR (CD_3CN , 300 MHz): δ 5.94 (app t, $J = 2.1$ Hz, 2H, Cp), 5.68 (app t, $J = 2.2$ Hz, 2H, Cp), 3.56–3.50 (m, 2H, $\text{CH}_2\text{CH}_2\text{N}$), 3.12 (s, 9H, CH_3), 3.07–3.02 (m, 2H, $\text{CH}_2\text{CH}_2\text{N}$). $^{13}\text{C}\{^1\text{H}\}$ NMR (CD_3CN , 75 MHz): δ 224.8 (s, *trans* CO), 212.2 (s, *cis* CO).

$[\text{MoCH}_3(\text{CO})_3(\eta^5\text{-Cp}^{\text{NMMe}})]\text{I}$ (17). Yield: 49%. Anal. Calcd for $\text{C}_{14}\text{H}_{20}\text{NO}_3\text{Imo}$: C, 35.54; H, 4.26; N, 2.96. Found: C, 35.59; H, 4.32; N, 3.04. Mp: 143–144 °C dec. IR (CH_3CN): $\nu(\text{CO})$ 2018 (s), 1927 (s) cm^{-1} . IR (Nujol): $\nu(\text{CO})$ 2012 (s), 1941 (s), 1918 (s), 1897 (s) cm^{-1} . ^1H NMR (CD_3CN , 300 MHz): δ 5.53 (app t, $J = 2.1$ Hz, 2H, Cp), 5.34 (app t, $J = 2.1$ Hz, 2H, Cp), 3.56–3.48 (m, 2H, $\text{CH}_2\text{CH}_2\text{N}$), 3.14 (s, 9H, $\text{N}(\text{CH}_3)_2$), 2.78–2.68 (m, 2H, $\text{CH}_2\text{CH}_2\text{N}$), 0.36 (s, 3H, MoCH_3). $^{13}\text{C}\{^1\text{H}\}$ NMR (CD_3CN , 75 MHz): δ 241.1 (s, *trans* CO), 227.9 (s, *cis* CO), 109.6 (s, quat Cp), 95.0 (s, Cp), 92.4 (s, Cp), 67.2 (t, $J_{\text{NC}} = 2.9$ Hz, $\text{CH}_2\text{CH}_2\text{N}$), 54.0 (t, $J_{\text{NC}} = 3.9$, $\text{N}(\text{CH}_3)_2$), 22.7 (s, $\text{CH}_2\text{CH}_2\text{N}$), –19.3 (s, MoCH_3).

$[\text{WCH}_3(\text{CO})_3(\eta^5\text{-Cp}^{\text{NMMe}})]\text{I}$ (18). DME (200 mL) was added to $\text{W}(\text{CO})_6$ (1.21 g, 3.42 mmol) and NaCp^{N} (0.600 g, 3.77 mmol). The yellow solution was refluxed for 15 h. The THF was removed in vacuo, and the residue was dissolved in CH_3CN (100 mL). An aliquot of a 2.0 M CH_3I solution in *tert*-butyl methyl ether (4.2 mL, containing 1.2 g, 8.4 mmol of CH_3I) was added, resulting in a cloudy yellow solution; the $[\text{W}(\text{CO})_3(\eta^5\text{-Cp}^{\text{N}})]^-$ was consumed within 5 min. The suspension was filtered through alumina. The filtrate was concentrated in vacuo until ~5 mL remained. Addition of Et_2O (75 mL) precipitated a yellow solid. The solid was isolated by filtration, washed with Et_2O (4×20 mL), and dried in vacuo. Recrystallization ($\text{CH}_3\text{CN}/\text{Et}_2\text{O}$) provided pale yellow, moderately air-sensitive microcrystals (1.26 g, 66%). Anal. Calcd for $\text{C}_{14}\text{H}_{20}\text{NO}_3\text{IW}$: C, 29.97; H, 3.59; N, 2.50. Found: C, 30.21; H, 3.46; N, 2.62. Mp: 204–205 °C dec. IR (CH_3CN): $\nu(\text{CO})$ 2014 (s), 1917 (s) cm^{-1} . IR (Nujol): $\nu(\text{CO})$ 2007 (s), 1932 (s), 1886 (s) cm^{-1} . ^1H NMR (CD_3CN , 300 MHz): δ 5.65 (app t, $J = 2.1$ Hz, 2H, Cp), 5.43 (app t, $J = 2.1$ Hz, 2H, Cp), 3.58–3.51 (m, 2H, $\text{CH}_2\text{CH}_2\text{N}$), 3.15 (s, 9H, $\text{N}(\text{CH}_3)_2$), 2.83–2.77 (m, 2H, $\text{CH}_2\text{CH}_2\text{N}$), 0.41 (s, 3H, WCH_3). $^{13}\text{C}\{^1\text{H}\}$ NMR (CD_3CN , 75 MHz): δ 230.9 (s, *trans* CO), 217.8 (s, *cis* CO).

X-ray Crystallographic Characterization of 7–12 and 18. X-ray-quality crystals of 7–9 were obtained by diffusion of Et_2O into a DMSO solution of each compound. Crystals of 10–12 and 18 were obtained by diffusion of Et_2O into a CH_3CN solution of each compound. These crystals were selected from the mother liquor in a N_2 -filled glovebag.

Acknowledgment. The donors of the Petroleum Research Fund, administered by the American Chemical Society (ACS PRF 39928-GB3), and an award from Research Corp. (CC5932) supported this research. We are grateful to these agencies and Macalester College.

Supporting Information Available: Text, figures, and tables giving additional experimental details, ^{13}C NMR spectral data, and crystallographic data as well as data collection, solution, and refinement information for 7–12 and 18; crystallographic data are also given as CIF files. This material is available free of charge via the Internet at <http://pubs.acs.org>.

OM700497Z